

Neural hybrid tomograph for monitoring industrial reactors

Abstract. The article concerns research on the hybrid tomographic method, which simultaneously takes into account two types of tomography – ultrasonic tomography (UST) and electrical impedance tomography (EIT). An algorithm based on artificial neural networks (ANN) has been developed, the characteristic feature of which is the training of many regression neural networks. Each ANN output generates one of 4096 pixels of the reconstructed image. The inputs of neural networks are UST and EIT measurement vectors. Three variants of ANNs were trained: UST, EIT and a hybrid variant including UST and EIT measurements. Then the reconstruction results were compared. Surprisingly, the results of the performed experiments prove that the hybrid approach, i.e. the simultaneous use of UST and EIT measurements, does not always give better results than the use of a separate UST or EIT method. In the considered cases, when due to the nature of the examined object there are large differences in the quality of reconstruction between UST and EIT, the hybrid system tends to average the image. As a result, reconstructions from the hybrid system can be better than separate EIT but worse than separate UST.

Streszczenie. Artykuł dotyczy badań nad metodą tomografii hybrydowej, która jednocześnie uwzględni dwa rodzaje tomografii - ultradźwiękową (UST) i impedancyjną (EIT). Opracowano algorytm oparty na sztucznych sieciach neuronowych (ANN), którego charakterystyczną cechą jest wytrenowanie wielu regresyjnych sieci neuronowych. Każde wyjście ANN generuje jeden z 4096 pikseli zrekonstruowanego obrazu. Wejściami sieci neuronowych są wektory pomiarowe UST i EIT. Wytrenowano trzy warianty ANN: UST, EIT oraz wariant hybrydowy obejmujący pomiary UST i EIT. Następnie porównano wyniki rekonstrukcji. Co zaskakujące, wyniki przeprowadzonych eksperymentów dowodzą, że podejście hybrydowe, czyli jednoczesne zastosowanie pomiarów UST i EIT, nie zawsze daje lepsze rezultaty niż oddzielne zastosowanie metody UST lub EIT. W rozważanych przypadkach, gdy ze względu na charakter badanego obiektu występują duże różnice w jakości rekonstrukcji pomiędzy UST i EIT, system hybrydowy dąży do uśrednienia obrazu. W rezultacie rekonstrukcje z systemu hybrydowego mogą być lepsze niż czyste EIT, ale gorsze niż UST. (*Neuronowy tomograf hybrydowy do monitorowania reaktorów przemysłowych*).

Keywords: industrial tomography; machine learning; neural networks; hybrid systems.

Słowa kluczowe: tomografia przemysłowa, uczenie maszynowe, sieci neuronowe, systemy hybrydowe.

Introduction

This article presents the results of research on the combination of ultrasound tomography (UST) [1] and electrical impedance tomography (EIT) [2]. The mainstream of research has focused on developing an algorithm that allows obtaining tomographic images with the best resolution. There are many methods to solve optimization problems [3-7]. The system transforming the measurements into individual pixels of the output image was based on artificial neural networks (ANN).

Industrial tomography belongs to the group of non-invasive facility monitoring techniques. Another name for industrial tomography is process tomography. This type of tomography is successfully used in many industries. In particular, industrial tomography is used in the food, cosmetic, chemical, petroleum, pharmaceutical, metallurgical, waste disposal (biogas plants) and other industries.

The primary purpose of using process tomography is early failure detection and failure prevention. Another important purpose of using this type of tomography is the control of industrial processes. For example, due to the ability to detect crystals or gas bubbles formed in industrial reactors, process tomography enables the provision of necessary information in real time. In industrial reactors, phase changes take place in three states: solid, liquid and gas. If the correct course of the industrial process requires maintaining appropriate proportions between all three phases, this goal can be achieved with the use of industrial tomography.

Thanks to this information obtained from tomographic images with appropriate resolution, it is possible to make appropriate corrections and adjustments of the parameters of dynamic processes on an ongoing basis. As a consequence, effective monitoring of industrial processes enables their optimization in terms of time and cost as well as quality.

Invasive techniques are not the optimal solution for monitoring industrial processes because they have flaws. The first problem is that invasive measurement devices

affect the flow of the process by increasing uncertainty and reducing the level of control over the process. The dynamics of the process may be disturbed by invasive interference, which makes the process unstable and unpredictable.

Another problem with invasive monitoring methods can arise when dealing with indirect observation. Indirect observation consists in calculating the value of the monitored indicator on the basis of direct measurements of other physical quantities. As a result of process disturbances caused by the use of invasive methods and measuring devices, there is no guarantee that the mathematical formula used to calculate intermediate values will be correct.

Tomography is about solving the inverse problem based on measurement data. Natural predictions about ways to improve the quality, and in particular the resolution of tomographic images, are leading to increasing the number of measurement data. In connection with the above, a thesis can be made that if we combine data from two independent measurement methods, namely UST and EIT, the results should be better than for each of these methods used separately. The aim of the research is therefore to verify the hypothesis that hybrid tomography integrating both UST and EIT methods is more effective than homogeneous UST or EIT methods. The verification of this thesis consisted in the development of three algorithms based on artificial neural networks (UST + EIT, UST, EIT) and the verification of the above algorithms using a physical model.

Methods

The object of the research was a tank made of plastic. The EIT electrodes and UST transducers are placed alternately around the tank. The EIT electrodes are metal discs with an electric current of a certain intensity between them. The multiplexer ensured the appropriate changes of the electrode pairs to which the voltage was directed. UST transducers are transceivers. Due to the need to generate

sound waves and to receive them, transducers are complex electronic systems. Both the transducers and all other devices were designed in the research laboratory of Netrix SA. Figure 1 shows the view of the test stand for testing the effectiveness of the UST + EIT hybrid tomograph.



Fig.1. Test stand for UST+EIT hybrid tomograph [8]

The UST tomograph is visible on the left side of the tank, and the EIT tomograph on the right side.

Figure 2 shows the top view of the plastic transparent tank. In the middle there is a plastic tube filled with air. There are electrodes and transducers around the reservoir. During the experiments, the tank was filled with tap water.

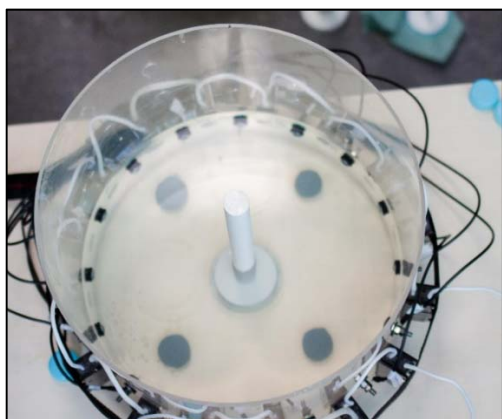


Fig.2. Tank with central inclusion

During the experiments, the arrangement of the tubes, their number and diameter were changed. Based on the obtained measurements, algorithms for simulating measurement data and corresponding model images were developed. Based on the simulation data, three independent neural network systems were trained for three types of tomographs - UST, EIT and the hybrid UST + EIT.

In order to train 3 variants of neural systems (UST, EIT and UST + EIT) measurements were performed using a hybrid tomograph [9-18]. Ultrasonic and electrical data were collected regarding identical allocation of inclusions within the tank reactor [19]. UST measurements were made using 16 transducers. The UST measurement vector had 120 values. EIT measurements were made using 16 sensors, thanks to which each measurement vector counted 96 measurements.

Figure 3 shows the view of the electronic system of the UST converter. As you can see, a complicated system is placed on the printed circuit board, which task is to emit ultrasonic signals with specific parameters of amplitude and frequency. Thanks to the use of a separate system with the task of generating signals, the UST system is flexible and programmable, especially in the aspect of emitting sound waves with various desired parameters. Receiving beeps is easier. A suitable microphone is sufficient for this.

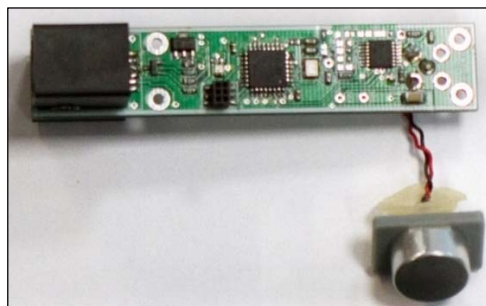


Fig. 3. The inside of the UST transducer

Scripts for generating simulation cases were developed on the basis of real measurements. The training set, for both UST and EIT, had 35000 cases. ANN structure for UST is (120-100-1)×4096. ANN structure for EIT is (96-100-1)×4096. ANN structure for UST+EIT is (216-200-1)×4096. Figure 4 shows a model of the UST+EIT hybrid system in a variant using a single ANN.



Fig. 4. The UST+EIT hybrid system converting 216 measurements with a single ANN

Previous experiments have shown that neural networks with fewer outputs learn better than networks with multiple outputs. Therefore, a solution has been applied in which each pixel of the output image is served by a separately trained ANN. Thanks to the use of a system of many neural networks, each of the 4096 ANNs generates one output signal, which is the value of image pixels. This variant is shown in Figure 5.

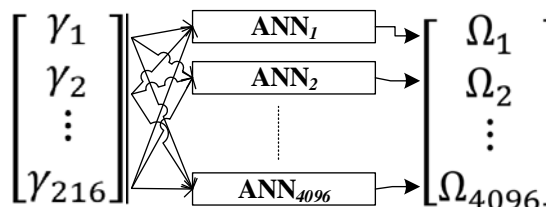


Fig. 5. The multiple ANN UST+EIT hybrid system converting 216 measurements into (64 × 64 = 4096 pixels) 2D image

Each of the 3 variants of the ANN models was trained on a training set, constituting 70% of all measurement cases. 15% of all cases was a test set and 15% a validation set.

The described problem of 2D tomographic images reconstruction is a classification problem. In order to show the presence of air-filled tubes placed inside a water-filled tank, a monochrome image, e.g. black and white, would be sufficient. Despite this, in the conducted experiments, it was decided to use neural regression networks that generate real numbers at the output. Although it causes blurring of the imaged shapes and the presence of color shades, it allows for a regressive analysis of the quality of the obtained reconstructions. Moreover, if binary classification networks are used, the images obtained would be highly noisy, since each misconstructed pixel is displayed in a contrasting manner, without varying the level of deviation from the background, which is tap water.

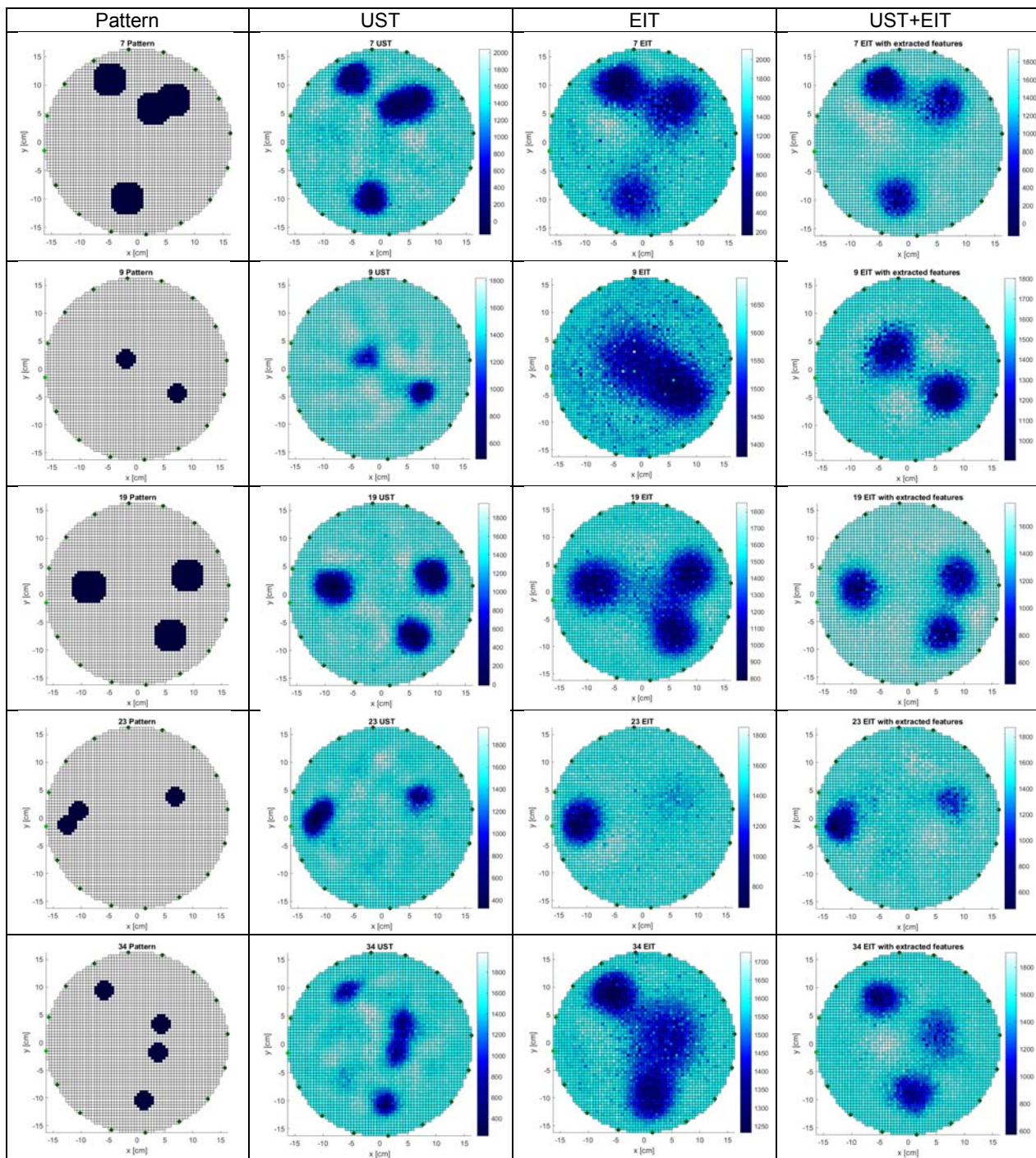


Fig. 6 Comparison of reconstruction images for 3 variants: UST, EIT and UST+EIT (hybrid)

Table 1. Comparison of image reconstruction metrics

Evaluation Metrics	Methods	Tested Cases					Mean
		#1	#2	#3	#4	#5	
ICC	EIT-UST	0.964	0.982	<u>0.986</u>	0.924	0.877	0.9466
	UST	<u>0.973</u>	<u>0.991</u>	0.984	<u>0.948</u>	<u>0.915</u>	
	EIT	0.721	0.682	0.813	0.761	<u>0.812</u>	
DE	EIT-UST	81.2	<u>68.6</u>	<u>79.3</u>	76.2	77.6	76.58
	UST	<u>80.6</u>	76.9	90.2	<u>74.2</u>	<u>74.5</u>	
	EIT	109.7	156.8	145.3	132.5	141.9	
RIE	EIT-UST	0.092	0.083	0.029	<u>0.064</u>	0.046	0.0628
	UST	<u>0.041</u>	<u>0.036</u>	<u>0.023</u>	0.07	<u>0.039</u>	
	EIT	0.106	0.189	0.044	0.115	0.142	

Results

Three indicators were used to quantitatively evaluate each of the tomographic methods. The first indicator was Image Correlation Coefficient (ICC), which was calculated according to the following formula (1):

$$(1) \quad ICC = \frac{\sum_{i=1}^n (\theta_i^* - \bar{\theta}^*) (\theta_i' - \bar{\theta}')}{\sqrt{\sum_{i=1}^n (\theta_i^* - \bar{\theta}^*)^2 \sum_{i=1}^n (\theta_i' - \bar{\theta}')^2}}$$

where: n - the number of pixels in the tomogram; $\bar{\theta}'$ - the mean value for reference pixels; $\bar{\theta}^*$ - the mean value for reconstructed pixels.

The second used indicator was Distribution Error (DE), which was calculated according to the formula (2):

$$(2) \quad DE = \frac{1}{n} \sum_{i=1}^n |\theta_i' - \theta_i^*|$$

where: θ_i' - the reference value of the pixel i ; θ_i^* - the reconstruction value of the pixel i .

The third used measure of the quality of the reconstructed images was Relative Image Error (RIE). The method of calculating the RIE indicator is determined by the formula (3):

$$(3) \quad RIE = \frac{\|\theta' - \theta^*\|}{\|\theta'\|}$$

The best image reconstructions should achieve high correlation coefficient ICC, minimum distribution error DE, and minimum image error RIE. Figure 6 shows the results of the reconstruction in a way enabling their comparison. Five selected measurement cases are presented in five lines. In the columns there are tomographic images showing in sequence: patterns, UST, EIT and UST + EIT (hybrid tomography). Table 1 presents the results of the reconstruction of individual variants for each of the five tested cases, using the ICC, DE and RIE indices.

Conclusions

The results of the conducted experiments prove that the hypothesis about the absolute advantage of the UST + EIT hybrid method over the UST or EIT homogeneous methods cannot be clearly confirmed. Analyzing the indicators for the five studied cases, we see that the large qualitative differences between UST and EIT image reconstructions mean that the hybrid combination of UST + EIT methods does not increase the quality of the reconstruction but averages it. As a consequence, the quality of the images generated by the UST + EIT hybrid tomograph gives way to the homogeneous UST tomography. On the other hand, in cases where the UST and EIT images are similar in terms of quality, the UST + EIT hybrid tomography is able to generate a synergy effect, thanks to which the hybrid image exceeds the quality of the images generated by the individual UST or EIT methods. Case study # 3 is proof of this.

A separate issue is the question of the individual characteristics of the research object. The results of the conducted research clearly indicate that better results were obtained with the UST. This does not mean, however, that the EIT method is generally inferior to UST, but it can be concluded that the plastic tank used during the experiments, filled with tap water, inside which plastic tubes filled with air were placed, is more susceptible to UST than EIT.

Authors: Grzegorz Kłosowski, Ph.D. Eng., Lublin University of Technology, Nadbystrzycka 38A, Lublin, Poland, E-mail: g.klosowski@pollub.pl; Tomasz Rymarczyk, Ph.D. Eng., University of Economics and Innovation, Projektowa 4, Lublin, Poland, E-mail: tomasz.rymarczyk@netrix.com.pl; Paweł Tchorzewski, Research & Development Centre Netrix S.A., Lublin, Poland, E-mail:

pawel.tchorzewski@netrix.com.pl; Piotr Bednarczuk, Ph.D. Eng., University of Economics and Innovation, Projektowa 4, Lublin, Poland; Marcin Kowalski, Ph.D. Eng., University of Economics and Innovation, Projektowa 4, Lublin, Poland;

REFERENCES

- [1] Rymarczyk T., Kozłowski E., Kłosowski G., Niderla K., Logistic Regression for Machine Learning in Process Tomography, *Sensors*, 19 (2019), No. 15, 3400
- [2] Rymarczyk T., Sikora J., Waleska B.: Coupled Boundary Element Method and Level Set Function for Solving Inverse Problem in EIT, 7th World Congress on Industrial Process Tomography, WC IPT7, 312-319, 2-5 September 2013, Krakow, Poland
- [3] Szczesny, A.; Korzeniewska, E. Selection of the method for the earthing resistance measurement. *Przegląd Elektrotechniczny*, 94 (2018), 178–181
- [4] Gałazka-Czarnecka, I.; Korzeniewska E., Czarnecki A. et al., Evaluation of Quality of Eggs from Hens Kept in Caged and Free-Range Systems Using Traditional Methods and Ultra-Weak Luminescence, *Applied sciences-basel*, 9 (2019), No. 12, 2430
- [5] Kosinski, T.; Obaid, M.; Wozniak, P.W.; Fjeld, M.; Kucharski, J. A fuzzy data-based model for Human-Robot Proxemics. In *Proceedings of the 2016 25th IEEE International Symposium on Robot and Human Interactive Communication (RO-MAN)*, New York, NY, USA, 26–31 August 2016; 335–340
- [6] Fraczyk, A.; Kucharski, J. Surface temperature control of a rotating cylinder heated by moving inductors. *Appl. Therm. Eng.* 2017, 125, 767–779
- [7] Kozłowski E., Mazurkiewicz D., Żabiński T., Prucnal S., Sęp J., Assessment model of cutting tool condition for real-time supervision system, *Eksploracja i Niezawodność – Maintenance and Reliability*, 21 (2019); No 4, 679–685
- [8] Kłosowski G., Rymarczyk T., Cieplak T., Niderla K., Skowron Ł., Quality assessment of the neural algorithms on the example of EIT-UST hybrid tomography, *Sensors*, 20 (2020), No. 11, 3324
- [9] Goetzke-Pala A., Hoła A., Sadowski Ł., A non-destructive method of the evaluation of the moisture in saline brick walls using artificial neural networks, *Arch. Civ. Mech. Eng.*, 18 (2018), No. 4, 1729–1742
- [10] Filipowicz S.F., Rymarczyk T., The Shape Reconstruction of Unknown Objects for Inverse Problems, *Przegląd Elektrotechniczny*, 88 (2012), No 3A, 55-57
- [11] Rymarczyk T., Adamkiewicz P., Duda K., Szumowski J., Sikora J., New Electrical Tomographic Method to Determine Dampness in Historical Buildings, *Archives of Electrical Engineering*, 65 (2016), No 2, 273-283
- [12] Rymarczyk T., New Methods to Determine Moisture Areas by Electrical Impedance Tomography, *International Journal of Applied Electromagnetics and Mechanics*, 52 (2016), 79-87
- [13] Rymarczyk T., Using electrical impedance tomography to monitoring flood banks, *International Journal of Applied Electromagnetics and Mechanics*, 45 (2014), 489–494
- [14] Rymarczyk T., Kłosowski G., Innovative methods of neural reconstruction for tomographic images in maintenance of tank industrial reactors. *Eksploracja i Niezawodność – Maintenance and Reliability*, 21 (2019); No. 2, 261–267.
- [15] Khairi M. T. M. et al., Ultrasound computed tomography for material inspection: Principles, design and applications, *Measurement*, 146 (2019), 490–523
- [16] Chen H. et al., Standard Plane Localization in Fetal Ultrasound via Domain Transferred Deep Neural Networks, *IEEE J. Biomed. Heal. Informatics*, 19 (2015), 1627–1636
- [17] Romanowski, A. Big Data-Driven Contextual Processing Methods for Electrical Capacitance Tomography. *IEEE Trans. Ind. Informatics*, 15 (2019), 1609–1618
- [18] Majchrowicz M., Kapusta P., Jackowska-Strumiłło L., Sankowski D., Acceleration of image reconstruction process in the electrical capacitance tomography 3d in heterogeneous, multi-gpu system, *Informatyka, Automatyka, Pomiar w Gospodarce i Ochronie Środowiska (IAPGOŚ)*, 7 (2017), No. 1, 37-41
- [19] Kłosowski G., Rymarczyk T., Kania K., Świć A., Cieplak T., Maintenance of industrial reactors based on deep learning driven ultrasound tomography, *Eksploracja i Niezawodność – Maintenance and Reliability*; 22 (2020), No 1, 138–147